International Journal of
Emerging Research in Management &Technology
ISSN: 2278-9359 (Volume-4, Issue-12)

Research Article | December 2015

A PMSG Based Wind Energy Conversion System: Modelling, Control and Stability Analysis

Duc Nguyen Huu*
Faculty of Energy Technology & Electric Power University,
Vietnam

Abstract—

This paper presents study on modeling, control system and stability analysis of a wind energy conversion system (WECS) with permanent magnet sysnchronous generator (PMSG). A WECS is combined with battery energy storage system (BESS) to provide better scheduled and flatten power to AC grid. Optimal generated power operation of this WECS is run follows on the maximal power point tracking method (MPPT). BESS and AC grid are operated according to a coordinated dc droop control. A state space model of the WECS is developed in detail to offer an in-depth insight into the system behaviors. The model can represent dynamics of wind turbine, generator and the converter-interfaced wind power plant around operating point. Second, a linearized model around operating point is obtained to provide a tool for stability analysis. Furthermore, this model can help for controller design. The dynamic performance of this configuration is evidenced by time-domain simulation with the state model of the system. Small signal stability is analyzed based on linearized model. Several analysis to investigate a selection of controller parameters is performed to realize effectiveness of the model.

Keywords— Wind Energy Conversion, PMSG, Battery Storage, Controller, Modelling, Stability

I. INTRODUCTION

Strong growth of renewable energy resource (RES) suggests that they will eventually be a substantial generation part of many electric power systems in the upcoming years. However, the rising penetration level poses the difficulty on operators because of their intermittency. A wind power plant can be operated in mission-critical networks especially for Vietnam, thus their stability assessment is required to investigate if the network is stable during transient events such as unexpected changes of wind speed. Furthermore, it is important to implement small-signal analysis with the control parameters of inverters during small disturbances. Therefore, the dynamic characteristics of such wind power plants for stability study and controller design are essential [1-2]. The state space method is well-known and introduced in many works [3]-[4]. The state space methodology makes possible study large-signal transient as well as small-signal stability. In [4] the state space averaging method applied into the dc analysis area of switching converters is discussed. This method proves fast, accurate and easy to implement in modeling the switching power converters. Thus, it is a good solution for small-signal analysis of such a wind power plant integrated with switching power converters.

This paper presents a state space representation of a PMSG based WECS with BESS in order to assess small signal stability in selection of controller parameters. The rest of this paper is organized as follows. Section 2 describes overall model of the system. Modeling of a WECS, BESS and an AC grid is presented in section 3. Section 4 introduces a MPPT applied to WECS and a coordinated droop for BESS and AC grid. Linearized model of the system is achieved in section 5. Simulations are carried out to realize effectiveness of the presented model in section 6. The conclusions are drawn in section 7.

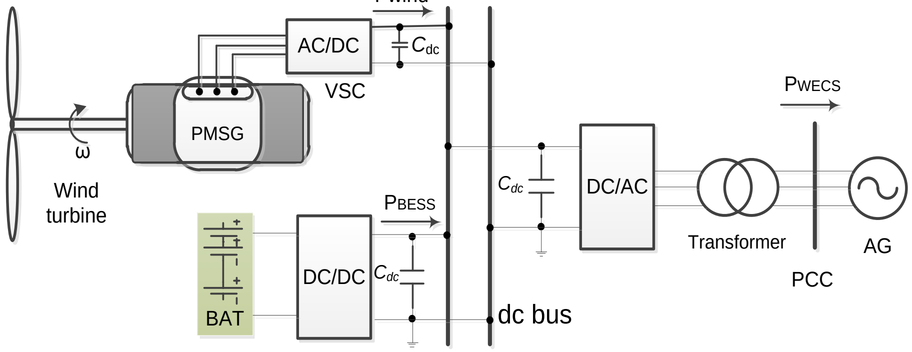

Fig. 1 Diagram of a PMSG based wind energy conversion system with battery energy storage connecting to AC grid

II. OUTLINE OF A WIND POWER PLANT

A schematic of the wind power plant with the conventions employed for power is shown in Fig. 1. The wind power plant is composed of a wind energy conversion system (WECS) and a battery energy storage system (BESS). WECS is connected to the dc bus through an AC/DC converter. BESS is integrated to the dc bus via a bi-directional buck converter.

Because of uncertainty wind, BESS is a significant device to effectively utilize or operate renewable energy from WECS. In this research, BESS is used to complement fluctuation of wind power from WECS in order to provide flatten power to AC grid. The WECS employs permanent magnet synchronous generator (PMSG). BESS of Vanadium Redox (VRB) is used because its power and capacity can be independently chosen. Therefore, the optimal capacity of BESS is designed. The wind power plant generates power to the AC grid through a transformer.

III. MODELING OF WIND POWER PLANT INTEGRATED TO AC GRID

A. Modeling of Electrical System of PMSG

The wind power generator employs permanent magnet synchronous generator (PMSG). With the MPPT (maximum power point tracking) control, the generator enables operation of the wind turbine at its maximum power coefficient over a wide range of wind speed thereby capturing a larger energy from the wind [5]. The voltage source ac/dc converter is used to connect PMSG to dc distribution. The state space model of the wind power generation unit is derived from [5]. The block diagram of the wind power generation unit is shown in Fig. 1.

The torque equations of PMSG can be written as follows:

$$\dot{\omega}_{\mathrm{r}} = \frac{1}{2H}(T_{\mathrm{m}} - T_{\mathrm{e}}) \tag{1}$$

where ω_r is rotor speed of PMSG, H is the inertia of PMSG, T_{m} and T_{e} is the mechanical torque and the electromagnetic of PMSG respectively. The d-q current equations describing the dynamic model of PMSG can be expressed as below.

$$\dot{i}_{\mathrm{d}} = \frac{1}{L_{\mathrm{md}} + L_{\mathrm{ls}}}(-R_{\mathrm{s}} i_{\mathrm{d}} + \omega_{\mathrm{e}}(L_{\mathrm{mq}} + L_{\mathrm{ls}}) i_{\mathrm{q}} + u_{\mathrm{d}}) \tag{2}$$

$$\dot{i}_{\mathrm{q}} = \frac{1}{L_{\mathrm{mq}} + L_{\mathrm{ls}}}(-R_{\mathrm{s}} i_{\mathrm{q}} - \omega_{\mathrm{e}}(L_{\mathrm{md}} + L_{\mathrm{ls}}) i_{\mathrm{d}} - \omega_{\mathrm{e}}\psi_{\mathrm{f}} + u_{\mathrm{q}}) \tag{3}$$

where subscripts d, q are respectively to the quantities of the d-axis, q-axis; the generator terminal voltage ud, uq can be stated as [5-7]:

$$u_{\mathrm{d}} = d_{\mathrm{d}} V_{\mathrm{dc}} \; ; \; u_{\mathrm{q}} = d_{\mathrm{q}} V_{\mathrm{dc}} \tag{4}$$

where d is the control signal applied to the converter; and V_{dc} is the dc bus voltage.

B. Modeling of Battery Energy Storage Systems

The energy storage system is composed of the battery and a dc/dc converter. The model of the battery introduced in [12]-[15] is adopted in this work. The battery storage system connected to dc bus is shown in Fig. 2.

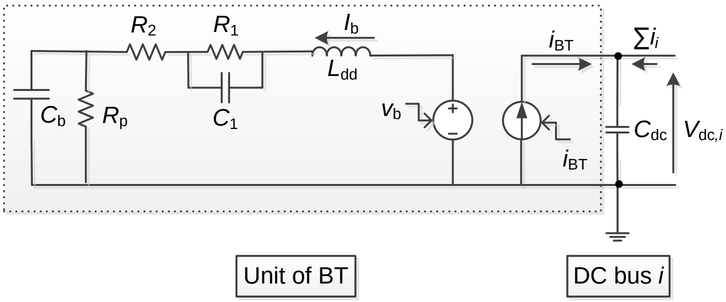

Fig. 2 Equivalent circuit of battery energy storage connecting to a dc bus

In order to develop state space representation of BESS, V_{cb} and V_{c1} are chosen as state variables. State equations describing dynamic behaviours of BESS can be expressed as follows.

$$\dot{I}_{\mathrm{b}} = \frac{1}{L_{\mathrm{dd}}}(-R_2 I_{\mathrm{b}} - V_{\mathrm{C1}} - V_{\mathrm{Cb}} + dV_i) \tag{5}$$

$$\dot{V}_{\mathrm{C1}} = \frac{1}{C_1}(I_{\mathrm{b}} - \frac{1}{R_1} V_{\mathrm{C1}}) \tag{6}$$

$$\dot{V}_{\mathrm{Cb}} = \frac{1}{C_{\mathrm{b}}}(I_{\mathrm{b}} - \frac{1}{R_{\mathrm{P}}} V_{\mathrm{Cb}}) \tag{7}$$

C. Modeling of AC Grid

Fig. 3(a) describes the circuit diagram of the AC grid integrated into the DC bus through an AC/DC rectifier, where R_{s} and L_{s} denote the equivalent resistance and inductance at the AC side. In order to facilitate the control design, the three-phase AC source in the abc-frame will be transferred into dq0 frame. Fig. 3(b) and (c) depict the equivalent circuits in d- and q-axis, in which e_{d} and e_{q} are the d- and q-axis voltage components of { $e_{\mathrm{a}}, e_{\mathrm{b}}, e_{\mathrm{c}}$ } in Fig. 3(b) and (c), and e_{q} is set to zero; L_{d} and L_{q} are the d- and q- axis inductance components of { $L_{\mathrm{sa}}, L_{\mathrm{sb}}, L_{\mathrm{sc}}$ }; R_{d} and R_{q} are the d- and q- axis resistance components of { $R_{\mathrm{sa}}, R_{\mathrm{sb}}, R_{\mathrm{sc}}$ }. Based on the equivalent circuit of AC grid integrated the wind power plant shown in Fig. 3, the voltage and current in dq0 coordinate system at the AC side have the following relationships with the voltage and current at the DC side:

$$\begin{aligned} v_{\mathrm{d}} &= d_{\mathrm{dAG}} V_{\mathrm{dc}} \\ v_{\mathrm{q}} &= d_{\mathrm{qAG}} V_{\mathrm{dc}} \\ I_{\mathrm{dc}} = i_{\mathrm{AG}} &= \frac{3}{2}(d_{\mathrm{dAG}} i_{\mathrm{dAG}} + d_{\mathrm{qAG}} i_{\mathrm{qAG}}) \end{aligned} \tag{8}$$

Therefore, the state equations of the AG unit can be expressed as:

$$\begin{aligned} \dot{i}_{\mathrm{dAG}} &= \frac{1}{L_{\mathrm{d}}}(-R_{\mathrm{s}} i_{\mathrm{dAG}} + \omega L_{\mathrm{s}} i_{\mathrm{qAG}} - d_{\mathrm{dAG}} V_i + e_{\mathrm{d}}) \\ \dot{i}_{\mathrm{qAG}} &= \frac{1}{L_{\mathrm{q}}}(-R_{\mathrm{s}} i_{\mathrm{qAG}} - \omega L_{\mathrm{s}} i_{\mathrm{dAG}} - d_{\mathrm{qAG}} V_i + e_{\mathrm{q}}) \\ \dot{V} &= \frac{1}{C_{\mathrm{dc}}}(\sum i_i + i_{\mathrm{AG}}) = \frac{1}{C_{\mathrm{dc}}}(\sum i_i + \frac{3}{2}(d_{\mathrm{dAG}} i_{\mathrm{dAG}} + d_{\mathrm{qAG}} i_{\mathrm{qAG}})) \end{aligned} \tag{9}$$

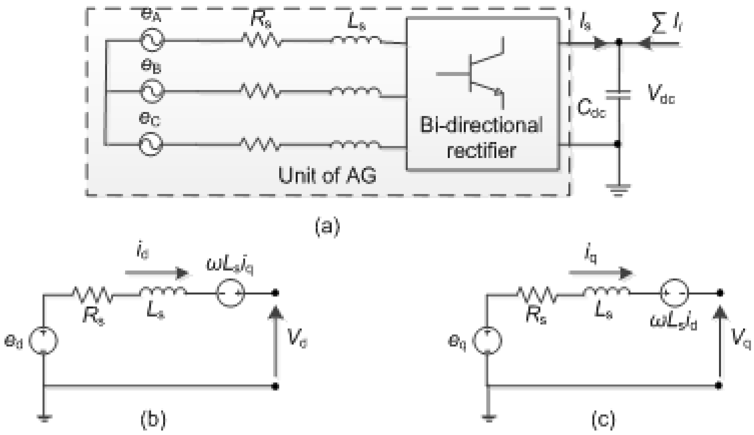

Fig. 3 Circuit diagram of AG unit and the equivalent circuits in (b) d- and (c) q axis

IV. CONTROL SYSTEMS

A. Control System of WECS

There are two control schemes for PMSG: speed controller and pitch angle controller [5]. The speed control is used to force the generator follow the predefined speed curve. The pitch angel control is aimed to prevent the generator from exceeding its rated power. When the wind speed is lower than its rated speed, the maximum power coefficient is maintained to capture maximum energy from wind. When the wind speed is high, the power coefficient is reduced by increasing the blade pitch angle to extract the maximum output power. The speed controller of the PMSG and the pitch angle controller of the wind turbine are depicted in Fig. 4 and Fig. 5 respectively.

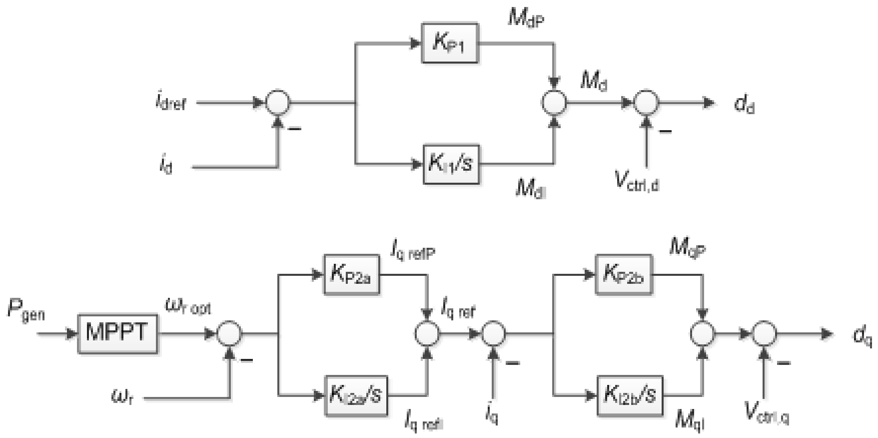

Fig. 4 Speed controller of the studied PMSG

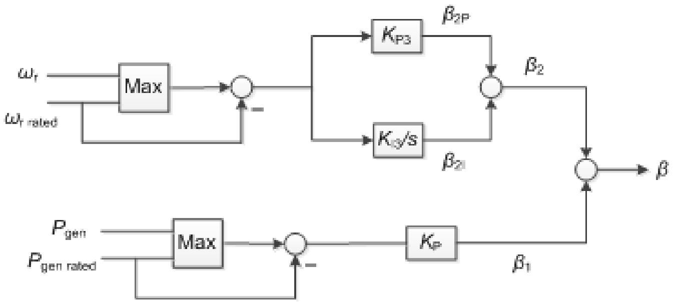

Fig. 5 Pitch angle controller of the wind turbine

Then, the state equations of the control system for wind power generation unit are developed as follows.

$$\dot{\beta}_{2I} = K_{I3}(\omega_r - \omega_{r\_rated}) \tag{10}$$

$$\dot{M}_{dI} = K_{I1}(i_{d\_ref} - i_d) \tag{11}$$

$$\dot{i}_{qrefI} = K_{I2a}(\omega_{r\_opt} - \omega_r) \tag{12}$$

$$\dot{M}_{qI} = K_{I2b}(i_{q\_ref} - i_q) \tag{13}$$

B. Coordinated Droop Control for BESS and AC grid

BESS and AC grid are operated in DC voltage droop control as depicted in Fig. 6(b). In the voltage range from $V_{dc,b-}$ to $V_{dc,b+}$, BESS is responsible for controlling dc voltage. By operating that, WECS with BESS can generate flatten power to AC grid. In the voltage range from $V_{dc,b+}$ to $V_{dc,max}$ and also from $V_{dc,b-}$ to $V_{dc,min}$, the droop curve of BESS is in saturation stage, thus the BESS supports at its maximum and constant. In addition, the dc/ac converter connecting to AC grid is stabilizing dc voltage when dc voltage in the range from $V_{dc,G+}$ to $V_{dc,max}$ and from $V_{dc,G-}$ to $V_{dc,min}$. It is noticed that these values of $V_{dc,G}$, $V_{dc,b}$ can be adjusted. The boundaries of $I_{B,max}$, $I_{B,min}$, $I_{G,max}$ and $I_{G,min}$ must respect the capacity of the respective converters.

In the unexpected disturbances in the AC grid, the AC grid is disconnected. Then, only BESS is responsible for controlling dc voltage. The control of the BESS converter is also described as discussed above. In accordance with this control scheme, generated power from WECS is stored in BESS within its capacity.

In Fig. 4(b), $I_{cor,b}$ and $I_{cor,AG}$ is corrective signals that are used for power allocation adjustments between BESS and AC grid. Here, $I_{d,b}$ is the signal taken from the DC droop control scheme, then it is summed up with the corrective signal $I_{cor,b}$. This signal is then sent through a current control loop to control BESS. The signal $I_{d,AG}$ is also taken from the DC droop scheme, then it is adjusted by summing up with the corrective signal $I_{cor,AG}$. $I_{d,AG}$ is then sent to a PI controller in the current control loop to control ac/dc converter connecting to AC grid.

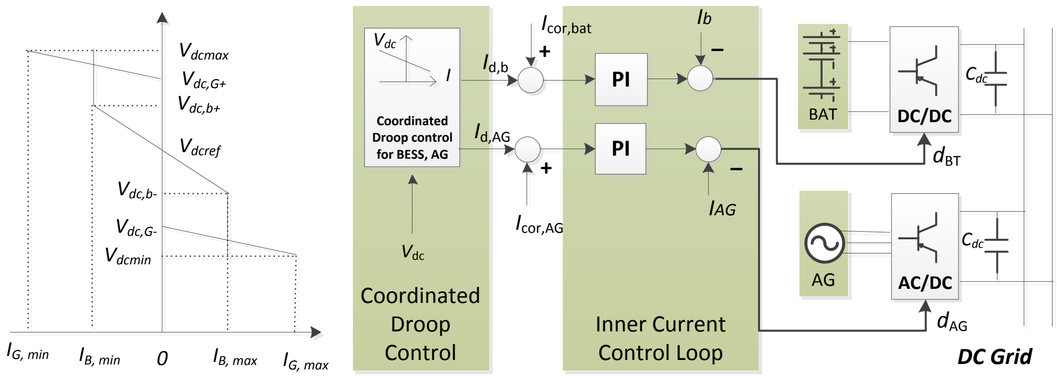

Fig. 6 (a) Coordinated droop control for BESS and AC grid; (b) Control diagram of BESS and AG units

The equations for PI controllers applied for BESS and AC grid are given as follows:

$$\begin{aligned} d_{\mathrm{PBT}} &= K_{\mathrm{PbBT}}(I_{\mathrm{b\_ref}} - I_{\mathrm{b}}) & d_{\mathrm{PAG}} &= K_{\mathrm{PbAG}}(I_{\mathrm{AG\_ref}} - I_{\mathrm{AG}}) \\ \dot{d}_{\mathrm{IBT}} &= K_{\mathrm{IbBT}}(I_{\mathrm{b\_ref}} - I_{\mathrm{b}}) & \dot{d}_{\mathrm{IAG}} &= K_{\mathrm{IbAG}}(I_{\mathrm{AG\_ref}} - I_{\mathrm{AG}}) \\ d_{\mathrm{BT}} &= d_{\mathrm{PBT}} + d_{\mathrm{IBT}} & d_{\mathrm{AG}} &= d_{\mathrm{PAG}} + d_{\mathrm{AGT}} \end{aligned} \tag{14}$$

where $I_{\mathrm{b\_ref}}$, $I_{\mathrm{AG\_ref}}$ are the reference currents achieved from the voltage control loop and $d_{\mathrm{BT}}, d_{\mathrm{AG}}$ are the average duty ratios of the converters; the subscript "P" and "I" represent the proportional and integral components of the duty ratio, respectively.

Those above state equations can be written as follows:

$$\mathbf{x} = \mathbf{f}(\mathbf{x},\mathbf{u},t) \tag{15}$$

where: $\mathbf{x}=\left[\mathbf{x}_{\text{WT}},\mathbf{x}_{\text{BESS}},\mathbf{x}_{\text{AG}}\right]^T$ is the state vector; $\mathbf{u}=\left[\mathbf{u}_{\text{WT}},\mathbf{u}_{\text{BESS}},\mathbf{u}_{\text{AG}}\right]^T$ is the input vector, *t* is the time.

V. LINEARIZATION MODEL, STABILITY ANALYSIS, CONTROLLER PARAMETER DESIGN

A. Linearization Model

In order to develop a linearized model of the system, three following main steps are carried out as follows.

Step 1: Calculate steady state values of the state vector at the operating point.

Step 2: Establish the small signal model of the sub-system including linearized model of PMSG, model of BESS and model of AC grid.

Step 3: Integrate linearized models of sub-systems into a compact linearized model of the system by superposition method.

With the input vector, the steady state values of the state vector can be determined by solving the following equation:

$$\mathbf{f}(\mathbf{x}_s,\mathbf{u}_s)=0 \tag{16}$$

So the steady state values of the output of the system can be achieved according to the equation as below:

$$\boldsymbol{y}_s=\boldsymbol{g}(\boldsymbol{x}_s,\boldsymbol{u}_s) \tag{17}$$

In step 2 the small signal model of the system will be established and defined as follows:

$$\dot{\tilde{\boldsymbol{x}}}=\boldsymbol{A}\tilde{\boldsymbol{x}}+\boldsymbol{B}\tilde{\boldsymbol{u}} \tag{18}$$

$$\tilde{\boldsymbol{y}}=\boldsymbol{C}\tilde{\boldsymbol{x}}+\boldsymbol{D}\tilde{\boldsymbol{u}} \tag{19}$$

where the small signals of the input vector, state vector and output vector can be written as:

$$\tilde{\mathbf{x}}=\mathbf{x}-\mathbf{x}_s\,;\tilde{\mathbf{u}}=\mathbf{u}-\mathbf{u}_s\,;\tilde{\mathbf{y}}=\mathbf{y}-\mathbf{y}_s \tag{20}$$

While the variables with "~" denote the small signals. The differential of the small signal is the same to that of the state variable because the differential of the constant steady state value is equal to zero. In accordance with Taylor Expansion **Error! Reference source not found.**], the matrices can be developed from:

$$\dot{\tilde{\mathbf{x}}}=\mathbf{f}(\mathbf{x}_s,\mathbf{u}_s)+\left.\frac{\partial\mathbf{f}}{\partial\mathbf{x}}\right|_{(\mathbf{x},\mathbf{u})=(\mathbf{x}_s,\mathbf{u}_s)}\times\tilde{\mathbf{x}}+\left.\frac{\partial\mathbf{f}}{\partial\mathbf{u}}\right|_{(\mathbf{x},\mathbf{u})=(\mathbf{x}_s,\mathbf{u}_s)}\times\tilde{\mathbf{u}}+\ldots \tag{21}$$

$$\tilde{\mathbf{y}}=\mathbf{g}(\mathbf{x}_s,\mathbf{u}_s)-\mathbf{y}_s+\left.\frac{\partial\mathbf{g}}{\partial\mathbf{x}}\right|_{(\mathbf{x},\mathbf{u})=(\mathbf{x}_s,\mathbf{u}_s)}\times\tilde{\mathbf{x}}+\left.\frac{\partial\mathbf{g}}{\partial\mathbf{u}}\right|_{(\mathbf{x},\mathbf{u})=(\mathbf{x}_s,\mathbf{u}_s)}\times\tilde{\mathbf{u}}+\ldots \tag{22}$$

where the matrix A, B, C, D can be defined as follows.

$$\mathbf{A}=\left.\frac{\partial\mathbf{f}}{\partial\mathbf{x}}\right|_{\mathbf{x}_s,\mathbf{u}_s};\ \mathbf{B}=\left.\frac{\partial\mathbf{f}}{\partial\mathbf{u}}\right|_{\mathbf{x}_s,\mathbf{u}_s};\ \mathbf{C}=\left.\frac{\partial\mathbf{g}}{\partial\mathbf{x}}\right|_{\mathbf{x}_s,\mathbf{u}_s};\ \mathbf{D}=\left.\frac{\partial\mathbf{g}}{\partial\mathbf{u}}\right|_{\mathbf{x}_s,\mathbf{u}_s} \tag{23}$$

Based on matrix A, B, C, D, the eigenvalues of the system can be calculated. The characteristic equation of A is defined as:

$$\det(\mathbf{A}-\lambda\mathbf{I})=0 \tag{24}$$

where $\mathbf{I}$ is an identity matrix of appropriate dimensions and λ is one of the system eigenvalues of the matrix A. If one of the eigenvalues of the matrix A has positive real part or is located on the right half of the complex plane, the system can be unstable for small disturbances.

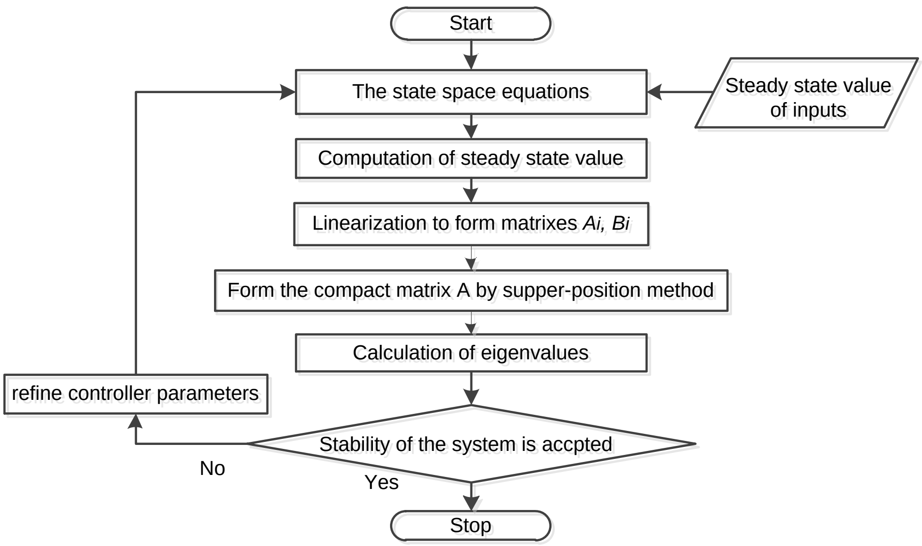

Fig. 7 The algorithm to select controller parameters using the small-signal model

Afterwards, based on this linearized model, a method to select parameters of controllers considering small-signal stability of the system is introduced as shown in Fig. 7.

VI. SIMULATION RESULTS

In this paper, several first simulations were implemented. State space representation of a PMSG based wind power plant is developed in Matlab. Verification of this model is realized by PSCAD/EMTDC. Afterwards, this model is used to investigate small signal stability of this system when there are small disturbances from changes of wind speed. The effects of controller parameters on stability are analyzed. In this study system as shown in Figure 1, the AC/DC converter connecting with AC grid and the DC/DC converter connecting to BESS are responsible for controlling DC voltage at DC bus according to the coordinated dc voltage droop control, the control system of the wind power plant is operated within the MPPT method to harvest maximal-clean energy from wind.

Simulation 1: Verification of the wind power plant with MPPT control scheme

State space model of a PMSG based wind power plant is developed in Matlab and verified by PSCAD/EMTDC. Case study is to simulate transients of a wind power plant with the MPPT control scheme. The control scheme circuit of the wind power generation unit is depicted in Fig. 4 and Fig. 5. The parameters of the simulation circuit are provided in Appendix. The simulation results for verification of the WECS model with its control scheme is shown in Fig. 8. Simulation results in Matlab are well matched with those of PSCAD/EMTDC as shown in Fig. 8. As a result, this model could be used for further analysis.

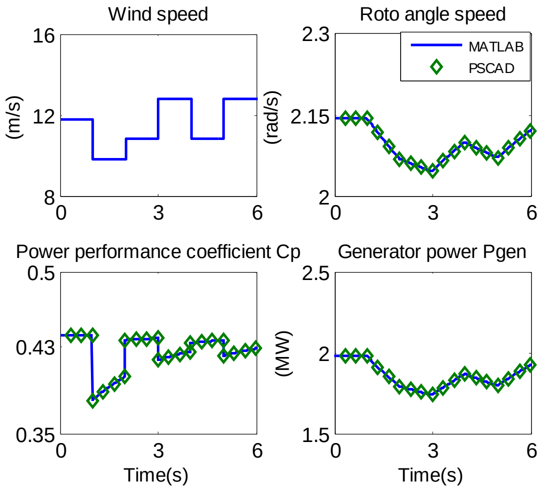

Fig. 8. Simulation results of the wind power generation unit with MPPT method

Simulation 2: Stability analysis of the system

Fig. 9 describes eigenvalues of the system. It is seen that all real magnitudes of the system eigenvalues are negative and in the left side of the plane, thus the system is stable under small-disturbances. However, it is analyzed that eigenvalues from converters close to the imaginary axis and eigenvalues from mechanical-electric process far from the imaginary axis. Therefore a selection of the controller parameters for converters is essential for the system stability. As a consequence, several following simulations are carried out to analyze effects of controller parameters on the system stability.

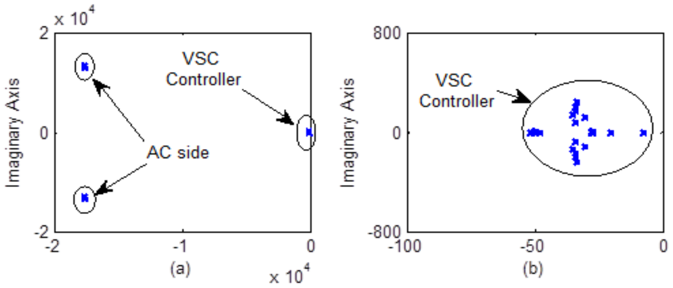

Fig. 9 Eigenvalues of the system

Simulation 3: Analyzing effect of the controller parameter K_{pa} in the DC/DC converter on stability

Parameter K_{pa} in the DC/DC converter connecting with BESS is important to control DC voltage at DC bus in order to keep a wind power plant working according to the MPPT control scheme. Higher K_{pa} could provide better voltage regulation but also could negatively affect to the system stability. Therefore, the value of K_{pa} should be investigated and selected properly. It is also necessary to analyze the system stability when designing the K_{pa}. Due to its importance, analyzing of K_{pa} will be performed as an illustrative example for proving the effectiveness of the spate space representation method.

To see the influence of the K_{pa}, locus of the system eigenvalues when value of the controller parameter in DC/DC converter connecting to BESS changes from 1 to 30 is depicted in Fig. 10. It is seen that the eigenvalues in the real axis are the same no matter how large the control gain K_{pa} is. However, with the increase of the control gain, the magnitude of eigenvalues in the imaginary axis will grow up dramatically, which may result in the larger oscillations in the transients. Because of all eigenvalues at the left side, the system is considered as stable.

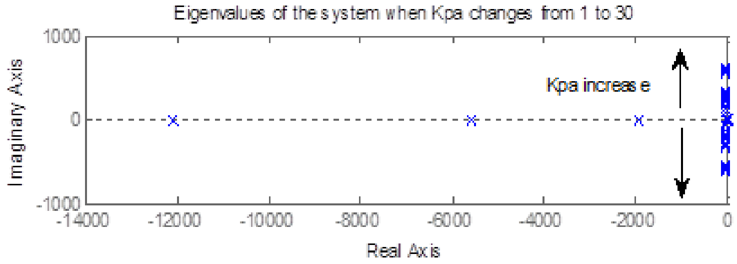

Fig. 10 Locus of eigenvalues when controller parameter Kpa in DC/DC converter connecting to BESS changes from 1 to 30

Simulation 4: Analyzing selection of K_{ia} in the DC/DC converter connecting to BESS

Locus of some important eigenvalues when K_{ia} in the DC/DC converter increases is shown in Fig. 11 When value of K_{ia} = 0.157, several eigenvalues move to the right plane, thereby leading to the system is unstable under small-disturbances.

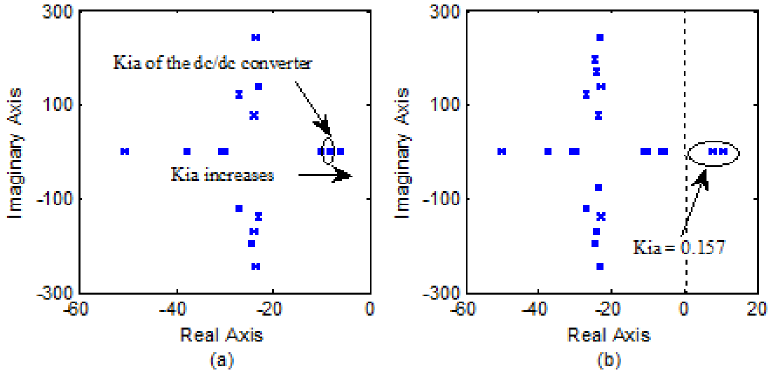

Fig. 11 Locus of eigenvalues when controller parameter Kia in DC/DC converter connecting to BESS increases

VII. CONCLUSIONS

A method for modeling the ensemble of a WECS including a wind turbine, PMSG, and VSC and BESS connecting to AC grid in the state space form that lend themselves to help stability analysis and control parameters selection was developed. The method is used as a useful tool to tuning their controller parameters. The overall method is composed of three main steps. First, a state space of each unit including turbine, PMSG, BESS and a simplified AC network is constructed. Second, linearization for all blocks was applied to provide small-signal analysis. The control employed for WECS tracks on maximum available wind power dynamically. The coordinated droop control applied for BESS and AC grid to control dc voltage at dc bus. Third, selection of several controller parameters was performed considering small-signal stability of the system. Therefore, it is essential to design a control scheme and controller parameters considering stability of the wind power plant connecting to AC grid. This model is especially necessary because of uncertainty of wind speed and power quality of electric networks in Vietnam.

APPENDIX: PARAMETERS FOR SIMULATION

Wind Energy Conversion System					
R_t	5 m / s	ρ	1.205kg/m^3	V_{wrated}	12m/s
K_{popt}	7.87W/(rad/s)^3	C_{pmax}	0.4412	$P_{genrated}$	2MW
ω_{rrated}	16.6rad/s	P	11	H	3 sec
Ψ_f	90 Wb	L_{md}	0.334H	L_{mq}	0.217H
L_{ls}	0.0344H	R_s	0.08Ω	K_{p1}	1.01/A
K_{i1}	2.21/A.s	K_{p2a}	5A/rad	K_{i2a}	150A/rad.s
K_{p2b}	1.01/A	K_{i2b}	2.21/A.s	K_{p3}	2deg/rad
K_{i3}	4deg/rad.s	C_{dcWT}	5 mF		
Battery Energy Storage System					
L_{ddBT}	120mH	C_{dcBT}	5 mH	R_{1BT}	0.1Ω
R_{2BT}	0.075Ω	R_{pBT}	25.10^{6}Ω	C_{1BT}	500F
C_{bBT}	300(F)	K_{p4aBT}	1 A / V	K_{i4aBT}	5A/V.s
K_{p4bBT}	0.3/A	K_{i4bBT}	2/A.s	V_{dcref}	480V
AC grid					
R_s	0.1 Ω	L_s	2.7 mH	E_s	6 kV
K_{pa}	3	K_{pb}	0.01	C_{dcAG}	3000F
K_{ib1}	0.2				

REFERENCES

[1] S. C. Smith, P. K. Sen, B. Kroposki, "Advancement of Energy Storage Devices and Applications in Electrical Power System," in Proc. 2008 IEEE Power and Energy Society General Meeting - Conversion and Delivery of Electrical of Electrical Energy in the 21th Century.

[2] H. Ibrahim, A. Ilinca, J. Perron, "Conversion and Analysis of Different Energy Storage Techniques Based on their Performance Index," in Proc. Electrical Power Conf. (EPC 2007), IEEE Canada, 2007.

[3] K. Qian, C. Zhou, Z. Li, Y. Yuan, "Benefits of Energy Storage in Power Systems with High Level of Intermittent Generation," in Proc. 20th International Conf. on Distribution - Part 1 (CIRED 2009). Prague, Czech Republic 2009.

[4] S. Faias, P. Santos, F. Matos, J. Sousa, R. Castro, "Evaluation of Energy Storage Devices for Renewable Energies Integration: Application to a Portuguese Wind Farm," in Proc. 5th International Conf. on European Electricity Market (EEM 2008), Libon, Portugal, 2008.

[5] Y. Li, D. Vilathamuwa, P. Loh, "Design, analysis, and real-time testing of a controller for multibus microgrid system," IEEE Trans. Power Electron.,vol. 19, 2004.

[6] N. Pogaku, M. Prodanovic, "Modeling, analysis, and testing of autonomous operation of an inverter-based microgrid," IEEE Trans. Power Electron., vol. 22, March 2007.

[7] L. O. Chua, P. M. Lin, "Computer-aided analysis of electronic circuits: Algorithms and Computational Techniques," Prentice-Hall, INC., Englewood Cliffs, New Jersey.

[8] M. Plesnik, "Use of the state-space averaging technique in fast steady-state simulation algorithms for switching power converters," IEEE CCECE/CCGEI, Ottawa, May 2006.

[9] N. P. W. Strachan, D. Jovcic, "Dynamic modeling, simulation and analysis of an offshore variable-speed directly-driven permanent-magnet wind energy conversion and storage system (WECSS)," OCEANS 2007-Europe, 18-21, Pages:1-6, June 2007.

[10] B. K. Bose, "Modern Power Electronics and AC drives," Upper Saddle River, NJ: Prentice Hall, chapter 2, 8, 5, 2001.

[11] A. Yzdani, R. Iravani, "A neutral-point clamped converter system for direct-drive variable-speed wind power unit," IEEE Trans. Energy Conversion., vol. 21, no. 2, page(s):596-607, Jun. 2006.

[12] Z. M. Salameh, M. A. Casacca, . A. Lynch," A mathematical model for lead-acid batteries,". IEEE Trans. Energy Conversion, vol. 7, no. 1, Page(s):93C98, Mar. 1992.

[13] D. Linden, Ed. ,"Handbook of batteries,". 2nded. New York: McGraw-Hill, 2001.

[14] C. T. Rim, N. S. Choi, G. C. Cho, "A complete dc and ac analysis of three-phase controlled-current PWM rectifier using circuit D-Q transformation,". IEEE Trans. On Power Electronics, vol. 9, No. 4. Page(s):390-396, July 1994.

[15] D. Nguyen Huu, "State Space Modelling and Voltage Control of AC-DC Networks," Ph.D. Thesis, Technical University of Berlin, 2014

